

Gap-K%: Measuring Top-1 Prediction Gap for Detecting Pretraining Data

Minseo Kwak

Yonsei University

rhkralstj103@yonsei.ac.kr

Jaehyung Kim

Yonsei University

jaehyungk@yonsei.ac.kr

Abstract

The opacity of massive pretraining corpora in Large Language Models (LLMs) raises significant privacy and copyright concerns, making pretraining data detection a critical challenge. Existing state-of-the-art methods typically rely on token likelihoods, yet they often overlook the divergence from the model’s top-1 prediction and local correlation between adjacent tokens. In this work, we propose Gap-K%, a novel pretraining data detection method grounded in the optimization dynamics of LLM pretraining. By analyzing the next-token prediction objective, we observe that discrepancies between the model’s top-1 prediction and the target token induce strong gradient signals, which are explicitly penalized during training. Motivated by this, Gap-K% leverages the log probability gap between the top-1 predicted token and the target token, incorporating a sliding window strategy to capture local correlations and mitigate token-level fluctuations. Extensive experiments on the WikiMIA and MIMIR benchmarks demonstrate that Gap-K% achieves state-of-the-art performance, consistently outperforming prior baselines across various model sizes and input lengths¹.

1 Introduction

Large Language Models (LLMs) have recently demonstrated remarkable capabilities, including understanding, reasoning, and generation tasks (OpenAI, 2024; Comanici et al., 2025). A key to this success is pretraining on massive-scale data, mostly collected through web crawling. However, the details of these pretraining corpora remain largely undisclosed for many state-of-the-art models (Yang et al., 2025; Grattafiori et al., 2024). This lack of transparency raises significant concerns, as pretraining data may contain Personally Identifiable Information (PII) (Lukas et al., 2023)

or copyrighted content (Rahman and Santacana, 2023), leading to ethical and legal issues. Moreover, if benchmark datasets are unknowingly included in the pretraining data, model performance would be inflated, leading to unfair comparisons (Oren et al., 2023).

For these reasons, *pretraining data detection* (Shi et al., 2024) has emerged as a critical problem; this problem is an instance of membership inference attack (MIA) (Shokri et al., 2017), which aims to determine whether a data point was in the training dataset. Representative state-of-the-art methods typically address this problem by exploiting token-level likelihoods. For instance, Min-K% (Shi et al., 2024) assumes that non-training samples contain outlier tokens with low log probabilities, thus utilizing the average log probability of the bottom K% tokens as a detection score. Min-K%++ (Zhang et al., 2025) further improves this method by normalizing scores relative to the mean and variance of the predicted next token distribution. However, these approaches treat each token independently, failing to exploit the local correlations between adjacent tokens. Moreover, existing methods overlook the divergence from the top-1 next-token prediction, thereby missing informative signals reflecting the model’s optimized target.

In this work, we propose **Gap-K%**, a novel pretraining data detection method grounded in the optimization dynamics of LLM pretraining. We leverage the insight that the next-token prediction objective explicitly forces the model to align its top-1 prediction with the ground truth. Consequently, while training samples exhibit minimal divergence from the top-1 prediction, unseen data frequently triggers *confident mispredictions*, cases where the model strongly favors a plausible candidate other than the target. Building on this observation, Gap-K% quantifies the normalized gap between the log probabilities of the top-1 predicted token and the target token, effectively penalizing such confident

¹The code is available at <https://github.com/meaoww/gap-k>.

mispredictions. Furthermore, to exploit the local correlations within the token sequence, we apply a sliding window to the scores over adjacent tokens, thereby mitigating token-level fluctuations.

We validate the effectiveness of Gap-K% through experiments on two representative benchmarks, WikiMIA (Shi et al., 2024) and MIMIR (Duan et al., 2024). On WikiMIA, Gap-K% consistently outperforms prior state-of-the-art methods across five evaluated models. Averaged over five models, in the original setting, Gap-K% yields absolute AUROC improvements of 9.7% over the average of the existing baselines and 2.4% over the strongest baseline, Min-K%++. In the paraphrased setting, it achieves absolute AUROC gains of 5.7% over the average of the existing baselines and 1.7% over Min-K%++. On the more challenging MIMIR benchmark, Gap-K% attains the highest average performance across multiple Pythia models, including the 1.4B, 2.8B, 6.9B, and 12B variants.

In summary, our contributions are as follows:

- We identify that the gaps between top-1 predictions and target tokens as an effective detection signal, grounded in the optimization dynamics of next-token prediction.
- We propose Gap-K%, a novel pretraining data detection method that leverages top-1 prediction gaps and aggregates token-level signals to capture local correlations between adjacent tokens.
- We achieve state-of-the-art performance on WikiMIA and MIMIR benchmarks across various model sizes and input lengths.

2 Related Works

Membership inference attacks. Membership Inference Attacks (MIAs) aim to determine whether a given data sample was included in the training set. Samples included in the training data are referred to as members, while samples not included are non-members. In the context of LLMs, MIAs have been widely used for quantifying memorization (Carlini et al., 2022) and privacy risks (Mireshghallah et al., 2022; Steinke et al., 2023), as well as for detecting data contamination (Oren et al., 2023) and exposure of copyrighted content (Duarte et al., 2024; Meeus et al., 2024). MIAs can be categorized into reference-based and reference-free methods. Reference-based methods (Carlini et al., 2021; Mireshghallah et al., 2022; Ye et al., 2022) use additional reference models that are trained on data from a similar distribution. However, ob-

taining reference models is costly and often impractical, especially for pretrained LLMs. Therefore, reference-free methods have gained attention recently. Reference-free methods typically rely on loss (Yeom et al., 2018), and are further improved by comparing it with losses on perturbed samples (Mattern et al., 2023) or calibrating using compression-based entropy (Carlini et al., 2021).

Pretraining data detection. Pretraining data detection is a specific instance of MIAs, where the objective is to infer whether a given text is included in the pretraining corpus of an LLM. Compared to standard MIAs, detecting pretraining data is more challenging because the data is seen only a few times within a massive corpus, resulting in weak memorization signals. Moreover, the lack of access to the pretraining data distribution makes it difficult to employ reference models (Shi et al., 2024). Prior work (Shi et al., 2024; Zhang et al., 2025) has focused on token-level probabilities and treats tokens independently. In contrast, we consider sequential dependencies in text and leverage top-1 predictions, which have received little attention in prior work.

3 Method

3.1 Preliminary

Problem definition. Let \mathcal{M} be an autoregressive language model trained on an unknown dataset \mathcal{D} . Given a text sequence $\mathbf{x} = [x_1, \dots, x_N]$, the goal is to determine whether \mathbf{x} is a member of the training set ($\mathbf{x} \in \mathcal{D}$) or not ($\mathbf{x} \notin \mathcal{D}$). Specifically, a detection method computes a membership score $s(\mathbf{x}; \mathcal{M})$, predicting $\mathbf{x} \in \mathcal{D}$ if $s(\mathbf{x}; \mathcal{M})$ exceeds a threshold λ . We adopt a gray-box setting, where the model’s output logits and token probabilities can be accessed, but the model parameters and gradients are not available.

Detection with token probabilities. Existing state-of-the-art methods, such as Min-K% (Shi et al., 2024) and Min-K%++ (Zhang et al., 2025), rely on the likelihood of tokens. Min-K% computes a membership score by averaging log probabilities of the lowest $k\%$ tokens:

$$\text{Min-K}(\mathbf{x}) = \frac{1}{|\mathcal{I}_k(\mathbf{x})|} \sum_{t \in \mathcal{I}_k(\mathbf{x})} \log p(x_t | x_{<t}), \quad (1)$$

where $\mathcal{I}_k(\mathbf{x})$ denotes the set of indices of the lowest $k\%$ probability tokens. Min-K%++ builds on the intuition that training tokens are located near local maxima of the likelihood landscape, and thus

have higher probabilities relative to other candidates in the vocabulary. Min-K%++ formulates this by normalizing log-likelihoods:

$$\text{Min-K}++(\mathbf{x}) = \frac{1}{|\mathcal{I}_k(\mathbf{x})|} \sum_{t \in \mathcal{I}_k(\mathbf{x})} z_t, \quad (2)$$

$$z_t = \frac{\log p(x_t | x_{<t}) - \mu_t}{\sigma_t}, \quad (3)$$

where $\mu_t = \mathbb{E}_{z \sim p(\cdot | x_{<t})} [\log p(z | x_{<t})]$ is the mean of the next-token log probability and $\sigma_t = \sqrt{\mathbb{E}_{z \sim p(\cdot | x_{<t})} [(\log p(z | x_{<t}) - \mu_t)^2]}$ is the standard deviation.

3.2 Motivation and Insight

To distinguish training data from non-training data effectively, we focus on the fundamental behavior of the next-token prediction objective; we hypothesize that *the primary fingerprint of training is in the alignment between the model’s top prediction and the ground truth*.

Gradient-level analysis. Consider the cross-entropy loss at step t , $\ell_t = -\log p(y_t | x_{<t})$, where y_t denotes the next token in the pretraining sequence. The gradient of the loss with respect to $\text{logit } s_t(v)$ for any token $v \in V$ is:

$$\frac{\partial \ell_t}{\partial s_t(v)} = p(v | x_{<t}) - \mathbb{1}[v = y_t]. \quad (4)$$

Crucially, the magnitude of the gradient for non-target tokens ($v \neq y_t$) is directly proportional to their probability $p(v | x_{<t})$. The token with the highest probability, $v_t^{\max} = \arg \max_v p(v | x_{<t})$, exerts the strongest gradient signal if it does not match the target y_t . Therefore, during the training process, the optimization algorithm aggressively penalizes cases where $v_t^{\max} \neq y_t$.

As a consequence of this optimization, for samples within the training set \mathcal{D} , the model learns to align its top-1 prediction with the target token by minimizing the gap between $\log p(v_t^{\max})$ and $\log p(y_t)$. In contrast, for unseen data $\mathbf{x} \notin \mathcal{D}$, the model cannot rely on memorized trajectories and instead predicts the next token based on learned syntactic and semantic correlations. While the model may assign high probability to a plausible token (v_t^{\max}), the target token (y_t) often diverges from this top prediction, as multiple valid continuations exist for a given context and the text represents only one specific realization among them. Thus,

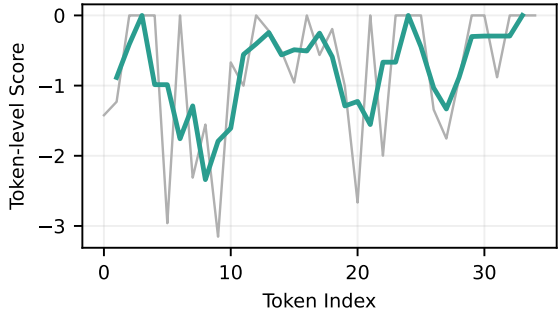


Figure 1: Illustration of token-level scores before and after sequential smoothing. The gray curve shows raw token-level scores, while the green curve shows the smoothed scores.

we hypothesize that a gap between the log probabilities of top-1 prediction and the target token serves as an informative signal to infer membership.

3.3 Proposed Method: Gap-K%

Building on the insight that training data exhibits minimal divergence between the top-1 prediction and the target token, we propose **Gap-K%**, a method designed to quantify this gap while accounting for sequential dependencies.

Top-1 gap scoring. First, we measure the token-level divergence. For each token x_t , we compute the difference between its log probability and the maximum log probability over the vocabulary (*i.e.*, the top-1 prediction). To account for the varying sharpness of the output distribution (*e.g.*, flat vs. peaked distributions), we normalize this difference by the standard deviation σ_t of the log probabilities, similar to Min-K%++:

$$g_t = \frac{\log p(x_t | x_{<t}) - \max_{v \in V} \log p(v | x_{<t})}{\sigma_t}. \quad (5)$$

Here, g_t is always *non-positive*; a value close to 0 indicates that the target token x_t has a log probability close to that of the top-1 prediction (highly likely for training data), while a large negative value indicates a significant divergence (likely for non-training data).

Sequential smoothing. Membership signals in LLMs are rarely isolated to a single token; they often span phrases or sentences, exhibiting sequential consistency due to the memorization of continuous text segments. To capture this local correlation and mitigate token-level fluctuations, we apply a

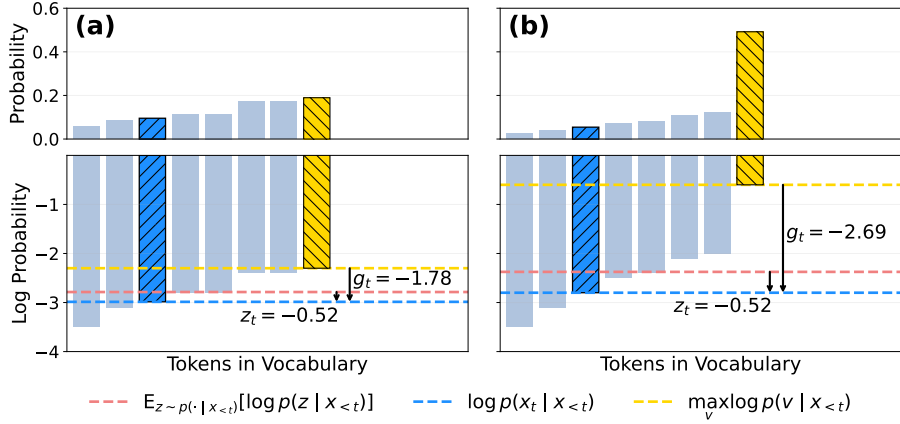


Figure 2: Conceptual comparison between Min-K%++ and Gap-K% using a toy example with a small vocabulary size of 8. Inspired by the illustrative analysis in Zhang et al. (2025), we compare the token-level scores of Min-K%++ (z_t) and Gap-K% (g_t) under two different next-token probability distributions. The z_t and g_t values annotated in the figure are normalized quantities as defined in the text. The blue hatched bar denotes the observed token x_t , while the yellow hatched bar indicates the top-1 token. In (a), the distribution is relatively flat, resulting in low-confidence incorrect predictions, whereas in (b) the model assigns high confidence to an incorrect top-1 token. While the Min-K%++ score z_t is identical in both cases, the Gap-K% score g_t distinguishes confident mispredictions from uncertain predictions by capturing the gap between the observed token and the distribution mode.

sliding window of size w over the gap scores:

$$\bar{g}_t^{(w)} = \frac{1}{w} \sum_{i=0}^{w-1} g_{t+i}. \quad (6)$$

As illustrated in Fig. 1, this smoothing step effectively highlights regions where the model consistently aligns (or fails to align) with the input text.

Gap-K% metric. Finally, following the principle of Min-K%, we focus on the *worst-case segments* that provide the strongest counter-evidence for membership. We define the Gap-K% score as the average of the lowest $k\%$ smoothed gap scores in the sequence:

$$\text{Gap-K\%}(\mathbf{x}) = \frac{1}{|\mathcal{I}_k(\mathbf{x})|} \sum_{t \in \mathcal{I}_k(\mathbf{x})} \bar{g}_t^{(w)}, \quad (7)$$

where $\mathcal{I}_k(\mathbf{x})$ denotes the set of token indices corresponding to the bottom- $k\%$ values of the smoothed scores $\{\bar{g}_t^{(w)}\}_{t=1}^{N-w+1}$. A higher Gap-K% score (closer to 0) implies that even the hardest-to-predict segments of the text exhibit minimal divergence from the model’s top-1 predictions, indicating membership in the training data.

3.4 Comparison with Min-K%++

To validate the advantage of Gap-K% over Min-K%++, we analyze the relationship between our scoring function g_t and the Min-K%++ score z_t . By

expanding Eq. 5 using the definition of z_t (Eq. 3), we can express g_t as:

$$g_t = z_t - \underbrace{\frac{\max_{v \in V} \log p(v | x_{<t}) - \mu_t}{\sigma_t}}_{\Delta_t}. \quad (8)$$

This formulation shows that our score differs from Min-K%++ by an additional term Δ_t , capturing the normalized gap between the top-1 log probability and the mean. It provides two critical insights.

Penalizing confident errors. Both methods focus on outlier tokens (lowest $k\%$ scores), which typically occur when the target token x_t differs from the top-1 prediction. In such scenarios, Min-K%++ (z_t) measures deviation solely from the mean, treating all low-probability tokens similarly regardless of the distribution shape. In contrast, Gap-K% (g_t) incorporates the confidence term Δ_t . Crucially, this allows our method to distinguish between *uncertain predictions* where the distribution is flat, and *confident mispredictions* where the model assigns high probability to an incorrect token, as illustrated in Fig. 2. By imposing a severe penalty on the latter, Gap-K% leverages these confident mispredictions as strong counter-evidence against membership; since training samples are optimized to eliminate such divergences, detecting these specific gaps provides a more robust signal for identifying non-training data than relying on likelihood alone.

Table 1: AUROC results on WikiMIA. *Ori.* and *Para.* indicate the original and paraphrased settings, respectively. **Bold** numbers denote the best performance.

Len.	Method	Mamba-1.4B		Pythia-6.9B		Pythia-12B		LLaMA-13B		LLaMA-65B		Average	
		Ori.	Para.										
32	Loss	61.0	61.3	63.8	64.1	65.4	65.6	67.5	68.0	70.8	71.9	65.7	66.2
	Zlib	61.9	62.3	64.4	64.2	65.8	65.9	67.8	68.3	71.2	72.1	66.2	66.6
	Neighbor	64.1	63.6	65.8	65.5	66.6	66.8	65.8	65.0	69.6	68.7	66.4	65.9
	Min-K%	63.3	62.9	66.3	65.1	68.1	67.2	66.8	66.2	70.6	70.1	67.0	66.3
	Min-K%++	66.4	65.7	70.3	67.6	72.2	69.4	84.4	82.7	85.3	81.6	75.7	73.4
	Gap-K%	69.2	67.2	71.4	68.1	73.7	70.2	86.8	83.7	88.0	82.5	77.8	74.3
64	Loss	58.2	56.4	60.7	59.3	61.9	60.0	63.6	63.1	67.9	67.9	62.5	61.3
	Zlib	60.4	59.1	62.6	61.6	63.5	62.1	65.3	65.3	69.1	69.5	64.2	63.5
	Neighbor	60.6	60.6	63.2	63.1	62.6	62.8	64.1	64.7	69.6	69.5	64.0	64.1
	Min-K%	61.7	58.0	65.0	61.1	66.5	62.5	66.0	63.5	69.9	66.8	65.8	62.4
	Min-K%++	67.2	62.2	71.6	64.2	72.6	65.1	84.3	78.8	83.5	74.3	75.8	68.9
	Gap-K%	69.9	64.3	73.3	66.7	74.8	67.1	87.2	81.2	86.7	76.7	78.4	71.2
128	Loss	63.3	62.7	65.1	64.7	65.8	65.4	67.8	67.2	70.8	70.2	66.6	66.0
	Zlib	65.6	65.3	67.6	67.4	67.8	67.9	69.7	69.6	72.2	72.2	68.6	68.5
	Neighbor	64.8	62.6	67.5	64.3	67.1	64.3	68.3	64.0	73.7	70.3	68.3	65.1
	Min-K%	66.8	64.4	69.5	67.0	70.7	68.5	71.5	68.6	73.8	70.5	70.5	67.8
	Min-K%++	67.7	63.3	69.8	65.9	71.8	67.7	83.8	76.2	80.8	70.0	74.8	68.6
	Gap-K%	71.2	67.4	71.5	66.2	75.0	69.5	85.7	79.4	83.6	70.7	77.4	70.6

Mode vs. Mean. From a statistical perspective, Min-K%++ assumes that training tokens are located near local maxima of the likelihood landscape. However, it adopts an *indirect* approach to capture this by measuring deviations from the *mean* of the vocabulary distribution. In contrast, Gap-K% aligns the metric with the assumption by directly measuring the divergence from the mode.

4 Experiments

In this section, we conduct comprehensive experiments to evaluate the proposed Gap-K%, designed to address the following research questions:

- **RQ1:** How effectively can Gap-K% detect pre-training data compared to existing baselines? (Table 1, 2 and Fig. 3)
- **RQ2:** How do the components of Gap-K% improve detection performance? (Table 3,4)
- **RQ3:** How do the different hyperparameters in Gap-K% affect the performance? (Fig. 4,5)
- **RQ4:** How does Gap-K% work differently from Min-K%++? (Fig. 6)

4.1 Setup

Benchmarks. We evaluate our method on WikiMIA (Shi et al., 2024) and MIMIR (Duan et al., 2024), two representative benchmarks for pretraining data detection. WikiMIA is constructed based on Wikipedia event pages and assigns training and non-training labels based on timestamps. WikiMIA provides both original and paraphrased

versions. Since detection difficulty may vary with input length, WikiMIA includes length-based splits. In our experiments, we evaluate the length splits of 32, 64, and 128 for both the original and paraphrased settings, following Zhang et al. (2025). MIMIR is a more challenging benchmark, designed to have minimal distributional differences between training and non-training samples. MIMIR is constructed from the Pile dataset (Gao et al., 2020) and consists of seven domains: English Wikipedia, GitHub, Pile-CC, PubMed Central, arXiv, DM Mathematics, and HackerNews.

Models. WikiMIA is constructed from Wikipedia, which is included in the pretraining data of many LLMs. Thus, we evaluate Mamba-1.4B (Gu and Dao, 2024), Pythia-6.9B and Pythia-12B (Biderman et al., 2023), LLaMA-13B and LLaMA-65B (Touvron et al., 2023). In contrast, MIMIR is designed for models trained on the Pile dataset. Following Duan et al. (2024), we evaluate Pythia-160M, 1.4B, 2.8B, 6.9B, and 12B.

Metrics. We evaluate the performance using the Area Under the ROC curve (AUROC) as our primary evaluation metric. AUROC captures the overall trade-off between the true positive rate (TPR) and false positive rate (FPR) across different thresholds. We also report the true positive rate at a low false positive rate (TPR@5%FPR).

Baselines. We compare our method with five state-of-the-art baselines: (1) *Loss* (Yeom et al.,

Table 2: AUROC results on MIMIR under the 13-gram 0.8 overlap setting (Duan et al., 2024). The best and second-best scores are highlighted in **bold** and underlined, respectively. For the Pythia-12B model, results for the Neighbor method are not reported due to computational constraints, consistent with Zhang et al. (2025).

Method	Wikipedia					Github					Pile CC					PubMed Central				
	160M	1.4B	2.8B	6.9B	12B	160M	1.4B	2.8B	6.9B	12B	160M	1.4B	2.8B	6.9B	12B	160M	1.4B	2.8B	6.9B	12B
Loss	50.2	51.3	51.8	52.8	53.5	<u>65.7</u>	69.8	71.3	73.0	71.0	49.6	50.0	50.1	50.7	51.1	49.9	49.8	49.9	50.6	51.3
Zlib	51.1	52.0	52.4	53.5	54.3	<u>67.5</u>	71.0	72.3	73.9	72.2	49.6	50.1	<u>50.3</u>	50.8	51.1	49.9	50.0	50.1	50.6	51.2
Neighbor	<u>50.7</u>	51.7	52.2	53.2	/	65.3	69.4	70.5	72.1	/	49.6	50.0	50.1	50.8	/	47.9	49.1	49.7	50.1	/
Min-K%	48.8	51.0	51.7	53.1	54.2	<u>65.7</u>	<u>70.0</u>	<u>71.4</u>	<u>73.3</u>	72.2	<u>50.1</u>	<u>50.5</u>	50.5	<u>51.2</u>	<u>51.5</u>	<u>50.3</u>	50.3	50.5	51.2	52.3
Min-K%++	49.2	<u>53.1</u>	<u>53.8</u>	<u>56.1</u>	<u>57.9</u>	64.7	69.6	70.9	72.8	73.8	49.7	50.0	49.8	<u>51.2</u>	<u>51.7</u>	50.2	<u>50.8</u>	<u>51.5</u>	<u>52.8</u>	54.0
Gap-K%	48.9	53.5	54.1	56.7	58.6	64.0	69.6	71.0	73.1	74.1	50.5	50.6	<u>50.3</u>	51.6	52.0	50.9	51.3	51.7	53.2	54.3
ArXiv					DM Mathematics					HackerNews					Average					
Method	160M	1.4B	2.8B	6.9B	12B	160M	1.4B	2.8B	6.9B	12B	160M	1.4B	2.8B	6.9B	12B	160M	1.4B	2.8B	6.9B	12B
Loss	51.0	51.5	51.9	52.9	53.4	48.8	48.5	48.4	48.5	48.5	49.4	50.5	51.3	52.1	52.8	52.1	53.1	53.5	54.4	54.5
Zlib	50.1	50.9	51.3	52.2	52.7	48.1	48.2	48.0	48.1	48.1	49.7	50.3	50.8	51.2	51.7	52.3	53.2	53.6	54.3	54.5
Neighbor	<u>50.7</u>	<u>51.4</u>	51.8	52.2	/	49.0	47.0	46.8	46.6	/	50.9	51.7	51.5	51.9	/	52.0	52.9	53.2	53.8	/
Min-K%	50.4	<u>51.4</u>	52.1	53.4	<u>54.3</u>	49.3	49.3	49.1	49.2	49.2	50.6	51.2	<u>52.4</u>	53.5	54.5	<u>52.2</u>	53.4	54.0	55.0	55.5
Min-K%++	49.3	50.9	<u>53.0</u>	53.6	56.2	50.1	50.2	50.5	50.4	50.7	51.3	52.6	<u>54.1</u>	55.8	52.0	<u>53.7</u>	<u>54.5</u>	<u>55.9</u>	57.1	
Gap-K%	49.9	51.5	53.3	53.8	56.2	50.0	49.9	49.9	50.2	50.1	50.2	51.2	52.2	54.2	55.6	52.1	53.9	54.6	56.1	57.3

2018) directly uses the input loss. (2) *Zlib* (Carlini et al., 2021) calibrates the loss using Zlib compression entropy. (3) *Neighbor* (Mattern et al., 2023) perturbs the input text using a pretrained masked language model and compares the loss of the original sample with the average loss of perturbed samples. (4) *Min-K%* (Shi et al., 2024) computes the average of the lowest K% token probabilities. (5) *Min-K%++* (Zhang et al., 2025) extends *Min-K%* by normalizing token-level log probabilities.

Implementation details. We use $k = 20\%$ for *Min-K%* following the setting in the original paper (Shi et al., 2024). To ensure a fair comparison across methods, we fix $k = 20\%$ for *Min-K%++* and *Gap-K%*. For *Gap-K%*, we set the window size to 6 for LLaMA-based models and 3 for other models, as these settings consistently showed stable and near-optimal performance across model sizes within each model family.

4.2 Main Results

WikiMIA results. Table 1 reports the AUROC scores on the WikiMIA benchmark. Overall, *Gap-K%* consistently outperforms existing methods across diverse settings. Averaged over five models, in the original setting, *Gap-K%* improves upon *Min-K%++* by 2.1%, 2.6%, and 2.6% for input lengths of 32, 64, and 128, respectively. For the paraphrased setting, *Gap-K%* also outperforms *Min-K%++* by 0.9%, 2.3%, and 2.0%. Moreover, the performance gains of *Gap-K%* generalize across a wide range of model sizes and architectures. We further report TPR@5%FPR results in

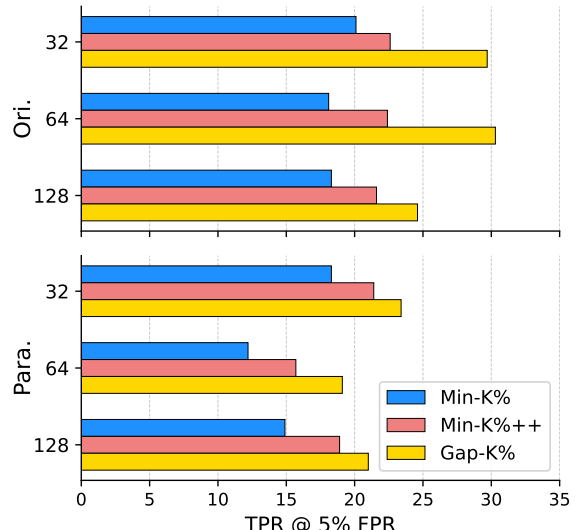


Figure 3: Average TPR@5% FPR across models for each evaluation setting (original vs. paraphrased inputs; sequence lengths of 32, 64, and 128). Full results are reported in Appendix A.

the Appendix A. Fig. 3 summarizes the average performance across input lengths. Among the baseline methods, *Min-K* and *Min-K%++* achieve the best overall performance in terms of AUROC, and we therefore focus on these two baselines in the main comparisons. As shown in Table 5, averaged over five models, *Gap-K%* substantially outperforms *Min-K%++* in the original setting, with gains of 7.1%, 7.9%, and 3.0% for input lengths of 32, 64, and 128, respectively. In addition, *Gap-K%* achieves an average gain of 2.5% in the paraphrased setting.

Table 3: Effect of sequential locality. Applying sequential smoothing improves performance only when the original token order is preserved.

Method	AUROC (%)
No smoothing	72.3
Shuffled-order smoothing	72.9
Sequential smoothing (Ours)	74.8

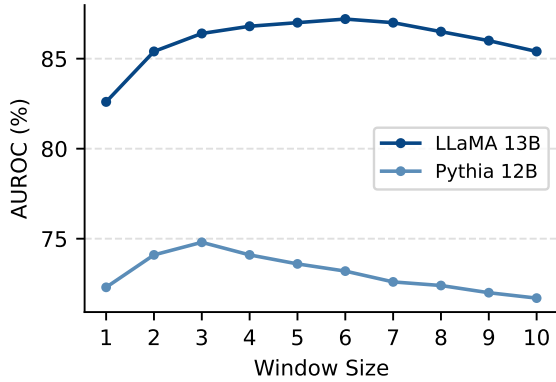


Figure 4: Effect of window size on sequential smoothing for LLaMA-13B and Pythia-12B.

MIMIR results. Table 2 reports the AUROC results on the MIMIR benchmark. MIMIR constitutes a particularly challenging membership inference benchmark, as member and non-member samples are drawn from the same distribution. As a result, the AUROC scores of most methods are close to random guessing (0.5), indicating the intrinsic difficulty of this setting. Despite this challenge, Gap-K% achieves the strongest performance on average across 1.4B, 2.8B, 6.9B, and 12B models. Notably, Gap-K% achieves higher average performance than Min-K%++ across the five evaluated model sizes. The TPR@5%FPR results are in the Appendix A.

4.3 Additional Analyses

We conduct additional analyses of Gap-K% on the WikiMIA-64 dataset using Pythia-12B.

Impact of window size. Fig. 4 presents the AUROC scores for window sizes ranging from 1 to 10 on LLaMA-13B and Pythia-12B. LLaMA-13B and Pythia-12B achieve their best performance at window sizes of 6 and 3, respectively, and the performance degrades for larger window sizes. As the window size increases, smoothing aggregates gap scores over a broader context, which may dilute localized high-gap regions that are indicative of

Table 4: Ablation of key components relative to Min-K%++. Top-1 denotes replacing the mean in Min-K%++ (Eq. 3) with the top-1 (maximum) log-probability, and smoothing denotes applying sequential smoothing.

Method	Top-1	Smoothing	AUROC (%)
Min-K%++			72.6
+ Top-1	✓		72.3
+ Smoothing		✓	73.8
Gap-K% (Ours)	✓	✓	74.8

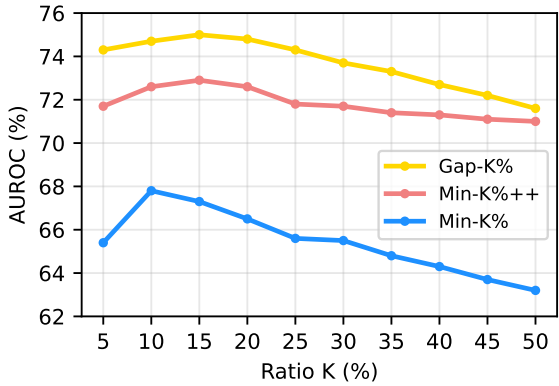


Figure 5: Effect of the $k\%$ ratio on AUROC.

non-training data.

Effect of sequential locality. To examine whether the effectiveness of sequential smoothing stems from local token dependencies, we compare three variants: (1) no smoothing, (2) smoothing applied after randomly shuffling the token order, and (3) sequential smoothing applied to the original token order (our method). As shown in Table 3, sequential smoothing leads to substantial improvements in AUROC only when the original token order is preserved. In contrast, applying the same smoothing operation after shuffling token order yields minimal improvement. This observation indicates that the membership signal exhibits sequential locality, with informative signals distributed across contiguous token segments rather than independently expressed at individual tokens.

Ablation of key components. We ablate the two key differences between our method and Min-K%++: Top-1 gap score in place of mean-based normalization and the application of sequential smoothing via a sliding window. Table 4 shows that neither modification alone is sufficient to achieve a large performance gain. Replacing the mean-based normalization with the Top-1 gap slightly degrades performance. On the other hand, applying sequential smoothing to the original Min-K%++

Text: The Exciters were an American pop music group of the 1960s. They were originally a girl group, with one male member being added afterwards. At the height of their popularity the group

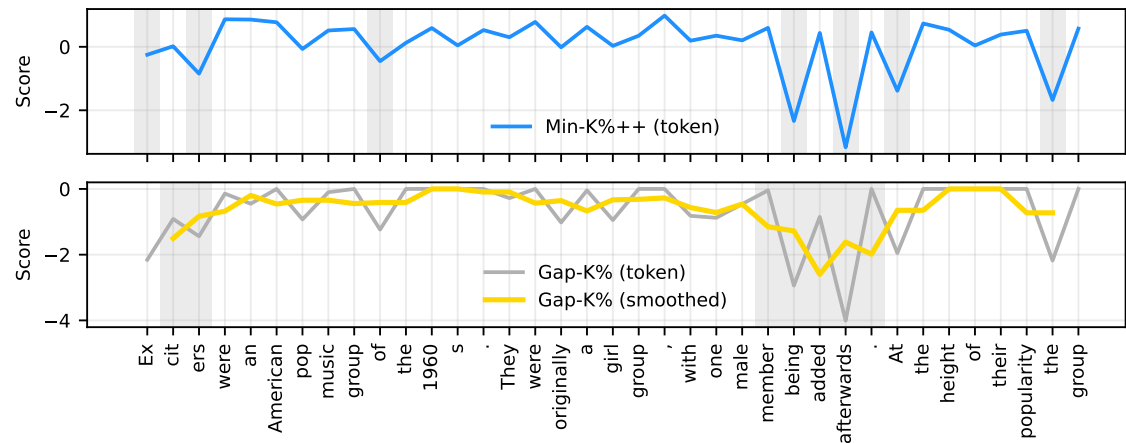


Figure 6: Visualization of token-level scores for Gap-K% and Min-K%++. Min-K%++ (top) selects tokens based on token-level scores, with shaded regions denoting the bottom 20% of tokens. Gap-K% (bottom) applies sequential smoothing to token-level scores and selects the bottom 20% based on the resulting window-averaged scores, which are indicated by shaded regions.

score leads to an improvement in AUROC, indicating that smoothing is generally effective. Importantly, the largest performance gain is achieved when sequential smoothing is applied to the Top-1 gap score. While smoothing alone stabilizes the score, the Top-1 gap provides a more discriminative per-token signal whose effectiveness is fully realized only after sequential smoothing.

Effect of $k\%$. Fig. 5 shows the effect of varying k from 5% to 50%. We observe that the performance peaks around $k = 15\%$. This trend suggests that selecting small $k\%$ tokens is effective for detection. This implies that focusing on tokens with larger log-probability gaps between the target token and the top-1 token yields stronger detection signals. Additionally, Gap-K% consistently outperforms Min-K% and Min-K%++ across the 5%–50% range, regardless of the choice of k .

Qualitative example. We analyze the behavior of token-level scores produced by Min-K%++ and Gap-K% to clarify how low-percentage selection mechanisms differ between the two methods. While the main quantitative experiments in prior sections are conducted on WikiMIA-64, we use WikiMIA-32 here for improved clarity in visualization. Fig. 6 is a corresponding visualization of token-level scores for a representative sample. Here, it is observed that Min-K%++ selects multiple low-scoring points distributed across the sequence, including both pronounced and minor low-score points. These selected points appear at iso-

lated positions rather than forming segments. In contrast, Gap-K% applies sequential smoothing before selecting the bottom $k\%$, which reflects score trends over neighboring tokens. As a consequence, the highlighted regions correspond to spans where scores remain relatively low across a short range, rather than isolated low-scoring points. This observation suggests that applying smoothing allows Gap-K% to capture low-score information at the level of local score patterns, while Min-K%++ operates directly on individual token-level values.

5 Conclusion

In this work, we studied pretraining data detection through the lens of the optimization dynamics of autoregressive large language models (LLMs). By analyzing the gradient behavior induced by the next-token prediction objective, we identified discrepancies between top-1 predictions and observed tokens as a meaningful signal for membership inference. Based on this insight, we proposed Gap-K%, a simple yet effective detection method that exploits top-1 log probability gaps and incorporates sequential smoothing to capture local correlations. Extensive experiments on the WikiMIA and MIMIR benchmarks demonstrate that Gap-K% consistently outperforms prior state-of-the-art methods. Overall, our findings highlight the importance of top-1 prediction behavior, together with sequential smoothing to capture local correlations. We hope this perspective motivates further exploration for understanding memorization, privacy risks in LLMs.

Limitations

Our method operates under a gray-box assumption, requiring access to token-level probability outputs from the target model. While this setting is common in prior work on pretraining data detection, it restricts the applicability of our approach to models or APIs that explicitly expose such information. Consequently, the method cannot be directly applied to fully black-box systems, including many commercial deployment scenarios.

In addition, our empirical evaluation focuses on representative and widely adopted model families that are commonly used in prior studies on pre-training data detection. However, these models do not include the most recent model families. As training regimes, data curation strategies, and architectural designs continue to evolve, the extent to which our findings generalize to newer model families remains an open question. Extending the evaluation to more recent architectures is therefore an important direction for future work.

Furthermore, while our experiments consider a paraphrased setting, we do not explicitly study adversarial settings in which paraphrases are deliberately optimized to evade detection. In particular, extremely aggressive or semantically obfuscated paraphrasing strategies that are designed with explicit knowledge of detection mechanisms may alter token-level statistics in ways that challenge our assumptions. Assessing the robustness of the proposed method under such intentional evasion scenarios remains unexplored and is left for future work.

Ethical Statements

This work is conducted with careful attention to ethical research practices and responsible use of data and models. The primary objective of our study is to improve the understanding of model behavior and privacy-related risks in LLMs. All experiments in this study are performed using publicly available datasets and pretrained models that are released for research purposes under permissive open-source licenses. Based on the available documentation provided by the dataset and model developers, the resources used in this work do not contain personally identifiable information (PII) and are commonly adopted benchmarks within the research community.

While our methods aim to enhance transparency and facilitate the detection of potential privacy risks

in pretrained models, we acknowledge that techniques could be misused if deployed irresponsibly. In particular, inferring characteristics of training data may pose risks when applied to sensitive or unauthorized data sources. To mitigate such concerns, we emphasize that our approach is intended strictly for non-commercial, academic research. Overall, this work aims to contribute to ongoing discussions on transparency and privacy considerations in LLMs.

References

Stella Biderman, Hailey Schoelkopf, Quentin Gregory Anthony, Herbie Bradley, Kyle O’Brien, Eric Hallahan, Mohammad Aflah Khan, Shivanshu Purohit, USVSN Sai Prashanth, Edward Raff, and 1 others. 2023. Pythia: A suite for analyzing large language models across training and scaling. In *Proceedings of the International Conference on Machine Learning (ICML)*, pages 2397–2430. PMLR.

Nicholas Carlini, Daphne Ippolito, Matthew Jagielski, Katherine Lee, Florian Tramer, and Chiyuan Zhang. 2022. Quantifying memorization across neural language models. In *International Conference on Learning Representations (ICLR)*.

Nicholas Carlini, Florian Tramer, Eric Wallace, Matthew Jagielski, Ariel Herbert-Voss, Katherine Lee, Adam Roberts, Tom Brown, Dawn Song, Ulfar Erlingsson, and 1 others. 2021. Extracting training data from large language models. In *30th USENIX security symposium (USENIX Security 21)*, pages 2633–2650.

Gheorghe Comanici, Eric Bieber, Mike Schaeckermann, Ice Pasupat, Noveen Sachdeva, Inderjit Dhillon, Marcel Blstein, Ori Ram, Dan Zhang, Evan Rosen, and 1 others. 2025. Gemini 2.5: Pushing the frontier with advanced reasoning, multimodality, long context, and next generation agentic capabilities. *arXiv preprint arXiv:2507.06261*.

Michael Duan, Anshuman Suri, Niloofar Mireshghallah, Sewon Min, Weijia Shi, Luke Zettlemoyer, Yulia Tsvetkov, Yejin Choi, David Evans, and Hannaneh Hajishirzi. 2024. Do membership inference attacks work on large language models? In *Conference on Language Modeling (COLM)*.

André Vicente Duarte, Xuandong Zhao, Arlindo L Oliveira, and Lei Li. 2024. De-cop: Detecting copyrighted content in language models training data. In *Proceedings of the International Conference on Machine Learning (ICML)*, pages 11940–11956. PMLR.

Leo Gao, Stella Biderman, Sid Black, Laurence Golding, Travis Hoppe, Charles Foster, Jason Phang, Horace He, Anish Thite, Noa Nabeshima, and 1 others. 2020. The pile: An 800gb dataset of diverse text for language modeling. *arXiv preprint arXiv:2101.00027*.

Aaron Grattafiori, Abhimanyu Dubey, Abhinav Jauhri, Abhinav Pandey, Abhishek Kadian, Ahmad Al-Dahle, Aiesha Letman, Akhil Mathur, Alan Schelten, Alex Vaughan, and 1 others. 2024. The llama 3 herd of models. *arXiv preprint arXiv:2407.21783*.

Albert Gu and Tri Dao. 2024. [Mamba: Linear-time sequence modeling with selective state spaces](#). In *Conference on Language Modeling (COLM)*.

Nils Lukas, Ahmed Salem, Robert Sim, Shruti Tople, Lukas Wutschitz, and Santiago Zanella-Béguelin. 2023. Analyzing leakage of personally identifiable information in language models. In *2023 IEEE Symposium on Security and Privacy (SP)*, pages 346–363. IEEE.

Justus Mattern, Fatemehsadat Mireshghallah, Zhijing Jin, Bernhard Schoelkopf, Mrinmaya Sachan, and Taylor Berg-Kirkpatrick. 2023. Membership inference attacks against language models via neighbourhood comparison. In *Findings of the Association for Computational Linguistics: ACL 2023*, pages 11330–11343.

Matthieu Meeus, Shubham Jain, Marek Rei, and Yves-Alexandre de Montjoye. 2024. Did the neurons read your book? document-level membership inference for large language models. In *33rd USENIX Security Symposium (USENIX Security 24)*, pages 2369–2385.

Fatemehsadat Mireshghallah, Kartik Goyal, Archit Uniyal, Taylor Berg-Kirkpatrick, and Reza Shokri. 2022. Quantifying privacy risks of masked language models using membership inference attacks. In *Conference on Empirical Methods in Natural Language Processing (EMNLP)*, pages 8332–8347.

OpenAI. 2024. [Hello gpt-4o](#).

Yonatan Oren, Nicole Meister, Niladri S Chatterji, Faisal Ladhak, and Tatsunori Hashimoto. 2023. Proving test set contamination in black-box language models. In *International Conference on Learning Representations (ICLR)*.

Noorjahan Rahman and Eduardo Santacana. 2023. Beyond fair use: Legal risk evaluation for training llms on copyrighted text. In *ICML Workshop on Generative AI and Law*.

Weijia Shi, Anirudh Ajith, Mengzhou Xia, Yangsibo Huang, Daogao Liu, Terra Blevins, Danqi Chen, and Luke Zettlemoyer. 2024. [Detecting pretraining data from large language models](#). In *International Conference on Learning Representations (ICLR)*.

Reza Shokri, Marco Stronati, Congzheng Song, and Vitaly Shmatikov. 2017. Membership inference attacks against machine learning models. In *2017 IEEE symposium on security and privacy (SP)*, pages 3–18. IEEE.

Thomas Steinke, Milad Nasr, and Matthew Jagielski. 2023. Privacy auditing with one (1) training run. *Advances in Neural Information Processing Systems (NeurIPS)*, 36:49268–49280.

Hugo Touvron, Louis Martin, Kevin Stone, Peter Albert, Amjad Almahairi, Yasmine Babaei, Nikolay Bashlykov, Soumya Batra, Prajjwal Bhargava, Shruti Bhosale, and 1 others. 2023. Llama 2: Open foundation and fine-tuned chat models. *arXiv preprint arXiv:2307.09288*.

An Yang, Anfeng Li, Baosong Yang, Beichen Zhang, Binyuan Hui, Bo Zheng, Bowen Yu, Chang Gao, Chengan Huang, Chenxu Lv, and 1 others. 2025. Qwen3 technical report. *arXiv preprint arXiv:2505.09388*.

Jiayuan Ye, Aadyaa Maddi, Sasi Kumar Murakonda, Vincent Bindschaedler, and Reza Shokri. 2022. Enhanced membership inference attacks against machine learning models. In *Proceedings of the 2022 ACM SIGSAC conference on computer and communications security*, pages 3093–3106.

Samuel Yeom, Irene Giacomelli, Matt Fredrikson, and Somesh Jha. 2018. Privacy risk in machine learning: Analyzing the connection to overfitting. In *2018 IEEE 31st computer security foundations symposium (CSF)*, pages 268–282. IEEE.

Jingyang Zhang, Jingwei Sun, Eric Yeats, Yang Ouyang, Martin Kuo, Jianyi Zhang, Hao Frank Yang, and Hai Li. 2025. [Min-k%++: Improved baseline for pre-training data detection from large language models](#). In *International Conference on Learning Representations (ICLR)*.

Table 5: TPR@5%FPR results on WikiMIA. The best and second-best scores are highlighted in **bold** and underlined, respectively.

Len.	Method	Mamba-1.4B		Pythia-6.9B		Pythia-12B		LLaMA-13B		LLaMA-65B		Average	
		Ori.	Para.										
32	Loss	14.2	14.2	14.2	15.0	17.1	17.3	14.0	<u>16.3</u>	22.0	21.7	16.3	16.9
	Zlib	<u>15.5</u>	13.2	16.3	12.7	17.1	15.5	11.6	15.0	19.6	17.3	16.0	14.7
	Neighbor	11.9	7.2	<u>16.5</u>	9.6	19.4	9.8	11.6	8.5	6.5	12.1	13.2	9.4
	Min-K%	14.2	11.9	17.8	21.7	<u>23.0</u>	19.9	18.9	14.2	26.4	23.8	20.1	18.3
	Min-K%++	11.4	7.8	14.5	14.5	16.5	15.5	<u>33.1</u>	33.9	<u>37.5</u>	35.4	<u>22.6</u>	<u>21.4</u>
	Gap-K%	17.3	<u>13.4</u>	16.3	<u>18.9</u>	24.0	<u>19.4</u>	43.4	33.9	47.3	<u>31.3</u>	29.7	23.4
64	Loss	9.5	8.1	13.4	10.6	9.2	11.6	11.3	12.0	15.5	13.4	11.8	11.1
	Zlib	14.1	15.1	16.2	15.8	11.3	16.2	12.7	13.4	17.6	18.3	14.4	<u>15.8</u>
	Neighbor	8.8	9.5	10.9	12.7	11.3	10.6	10.2	14.4	9.9	16.9	10.2	12.8
	Min-K%	<u>15.8</u>	7.7	<u>19.0</u>	12.7	<u>21.5</u>	12.7	17.3	13.4	16.9	14.4	18.1	12.2
	Min-K%++	13.7	7.0	16.2	10.2	16.9	10.9	<u>31.3</u>	<u>23.2</u>	<u>33.8</u>	27.1	<u>22.4</u>	15.7
	Gap-K%	20.1	<u>10.9</u>	23.6	<u>13.0</u>	25.4	<u>13.7</u>	44.7	30.3	37.7	27.8	30.3	19.1
128	Loss	11.5	<u>13.7</u>	14.4	16.5	18.0	19.4	21.6	18.0	20.1	24.5	17.1	18.4
	Zlib	19.4	17.3	20.9	20.9	23.7	19.4	18.7	21.6	23.0	22.3	21.1	<u>20.3</u>
	Neighbor	15.8	<u>13.7</u>	10.8	17.3	10.1	10.1	12.9	13.7	15.8	18.7	13.1	14.7
	Min-K%	9.4	5.0	18.0	16.5	20.1	18.7	20.1	15.1	<u>23.7</u>	19.4	18.3	14.9
	Min-K%++	10.1	6.5	<u>20.1</u>	<u>18.0</u>	18.0	<u>9.4</u>	<u>38.1</u>	35.3	21.6	<u>25.2</u>	<u>21.6</u>	18.9
	Gap-K%	<u>16.5</u>	<u>13.7</u>	19.4	13.7	<u>21.6</u>	18.0	39.6	<u>33.1</u>	25.9	26.6	24.6	21.0

Table 6: TPR@5%FPR results on MIMIR. The best and second-best scores are highlighted in **bold** and underlined, respectively.

Method	Wikipedia					Github					Pile CC					PubMed Central				
	160M	1.4B	2.8B	6.9B	12B	160M	1.4B	2.8B	6.9B	12B	160M	1.4B	2.8B	6.9B	12B	160M	1.4B	2.8B	6.9B	12B
Loss	4.2	4.7	4.7	5.1	5.0	22.6	32.1	33.6	38.5	30.3	3.1	<u>5.0</u>	4.8	4.9	5.1	4.0	4.4	4.3	4.9	5.0
Zlib	4.2	5.7	<u>5.9</u>	6.3	6.8	<u>25.1</u>	<u>32.8</u>	36.2	40.1	32.9	<u>4.0</u>	5.1	5.4	6.2	6.6	3.8	3.6	3.5	4.3	4.4
Neighbor	4.0	4.5	4.9	5.8	/	24.7	31.6	29.8	34.1	/	3.9	3.6	4.0	5.3	/	3.9	3.7	4.5	4.5	/
Min-K%	4.8	<u>5.6</u>	5.0	6.1	5.8	22.6	31.5	34.0	<u>39.0</u>	32.6	3.5	4.5	<u>4.8</u>	5.0	4.8	4.7	4.6	4.5	5.1	4.9
Min-K%++	5.2	<u>5.3</u>	5.9	<u>7.0</u>	7.8	25.2	33.0	34.2	38.2	<u>34.5</u>	5.0	3.7	3.7	4.8	4.6	4.8	6.1	<u>4.8</u>	<u>5.6</u>	6.4
Gap-K%	5.5	5.4	6.0	7.5	<u>7.0</u>	22.9	32.3	<u>34.3</u>	38.5	34.8	3.7	4.6	4.3	<u>5.8</u>	<u>5.9</u>	5.4	<u>5.2</u>	5.4	5.7	5.8
Method	ArXiv					DM Mathematics					HackerNews					Average				
	160M	1.4B	2.8B	6.9B	12B	160M	1.4B	2.8B	6.9B	12B	160M	1.4B	2.8B	6.9B	12B	160M	1.4B	2.8B	6.9B	12B
Loss	4.0	4.8	4.6	5.4	5.6	3.8	4.3	4.1	4.1	4.0	<u>5.0</u>	4.8	5.5	5.9	6.8	6.7	8.6	8.8	9.8	8.8
Zlib	2.9	4.3	4.1	4.6	4.7	4.1	<u>5.0</u>	4.6	4.3	4.3	<u>5.0</u>	5.5	5.8	5.6	5.8	7.0	8.9	9.4	10.2	9.4
Neighbor	4.7	4.8	4.4	4.1	/	5.6	4.4	4.5	<u>4.5</u>	/	6.5	<u>5.2</u>	5.3	5.7	/	<u>7.6</u>	8.3	8.2	9.1	/
Min-K%	4.4	4.3	4.5	5.4	5.3	3.9	4.1	4.6	4.3	<u>4.6</u>	4.2	4.6	<u>5.7</u>	6.3	<u>6.1</u>	6.9	8.5	9.0	10.2	9.2
Min-K%++	5.4	4.7	6.1	6.8	7.0	4.4	4.8	5.4	4.5	<u>5.4</u>	4.4	3.5	4.6	5.7	7.8	<u>8.7</u>	9.2	10.4	10.2	
Gap-K%	<u>5.2</u>	4.1	<u>5.3</u>	<u>6.4</u>	<u>6.1</u>	4.2	5.2	<u>4.8</u>	5.3	5.4	3.8	3.9	5.1	<u>6.2</u>	5.1	7.2	<u>8.7</u>	<u>9.3</u>	10.8	10.0

A Full TPR@5%FPR Results

In this section, we report full TPR@5%FPR results on the WikiMIA and MIMIR benchmarks in Tables 5 and 6, respectively. For WikiMIA, Gap-K% consistently outperforms Min-K%++ across different input lengths. In the original setting, averaged over five models, Gap-K% improves upon Min-K%++ by 7.1%, 7.9%, and 3.0% for input lengths of 32, 64, and 128, respectively. In the paraphrased setting, Gap-K% also achieves gains of 2.0%, 3.4%, and 2.1% over Min-K%++ for the same input lengths. These results further demonstrate the robustness of Gap-K% across both original and paraphrased settings. For MIMIR, no single method consistently achieves the best performance

across all model sizes. Gap-K% attains the highest average performance in the Pythia-6.9B setting and achieves the second-best average scores for the 1.4B, 2.8B, and 12B models.

B Window Size for Other Models

We further evaluate the effect of window size across additional models. Following the experimental setup in Section 4.3, we use the WikiMIA-64 dataset. Due to the high computational cost, we do not include results for LLaMA-65B. Fig. 7 shows that both Mamba-1.4B and Pythia-6.9B achieve their best performance at a window size of 3, consistent with the results for Pythia-12B.

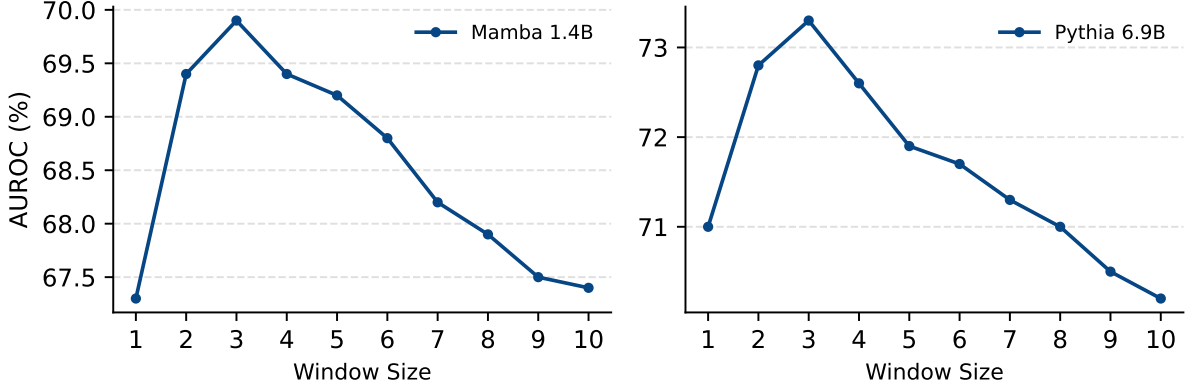


Figure 7: Effect of window size on sequential smoothing for Mamba-1.4B and Pythia-6.9B

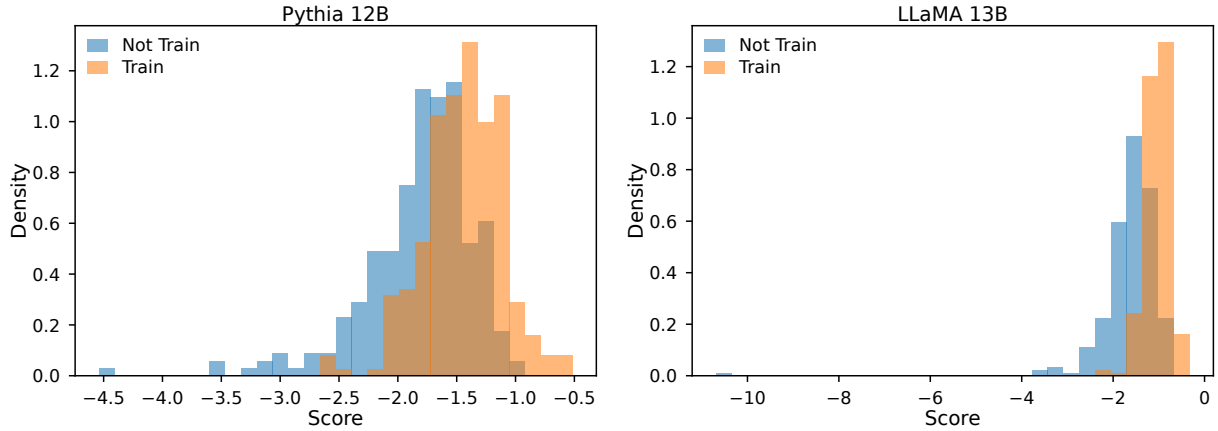


Figure 8: Histogram of the Gap-K% score distributions for trained and not trained samples on the WikiMIA-64 benchmark. The left shows results from Pythia-12B, and the right shows results from LLaMA-13B.

C Histogram-Based Comparison of Training and Non-Training Samples

Fig. 8 visualizes the distributions of the proposed Gap-K% scores for member and non-member samples. We plot the results for Pythia-12B and LLaMA-13B on the WikiMIA-64 benchmark. The histograms illustrate the degree of separation induced by the score.

D Additional Token-level Visualization

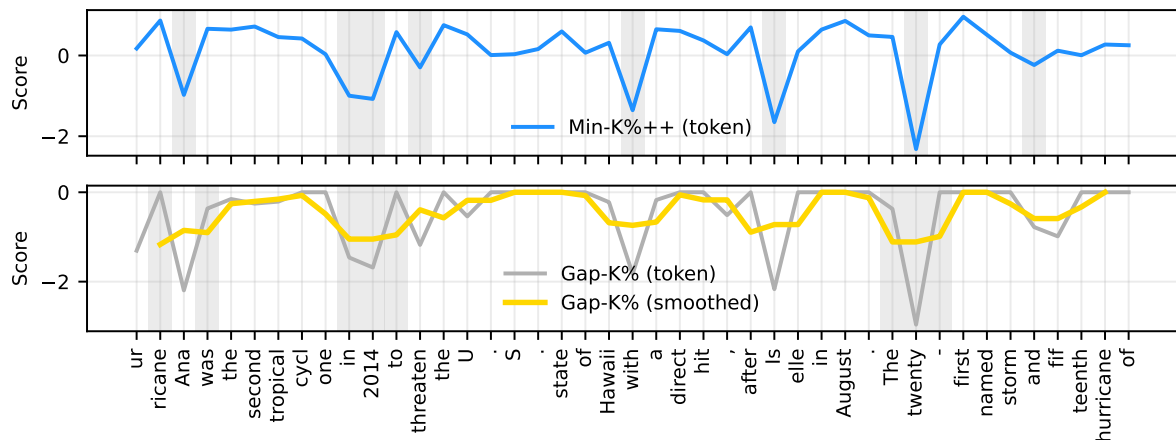
Fig. 9 presents additional qualitative examples of token-level score visualizations for Min-K%++ and Gap-K%. Consistent with the observation in Fig. 6 in the main text, Min-K%++ selects isolated low-scoring tokens across the sequence, whereas Gap-K% identifies contiguous low-score regions after applying sequential smoothing.

E Usage of AI assistants

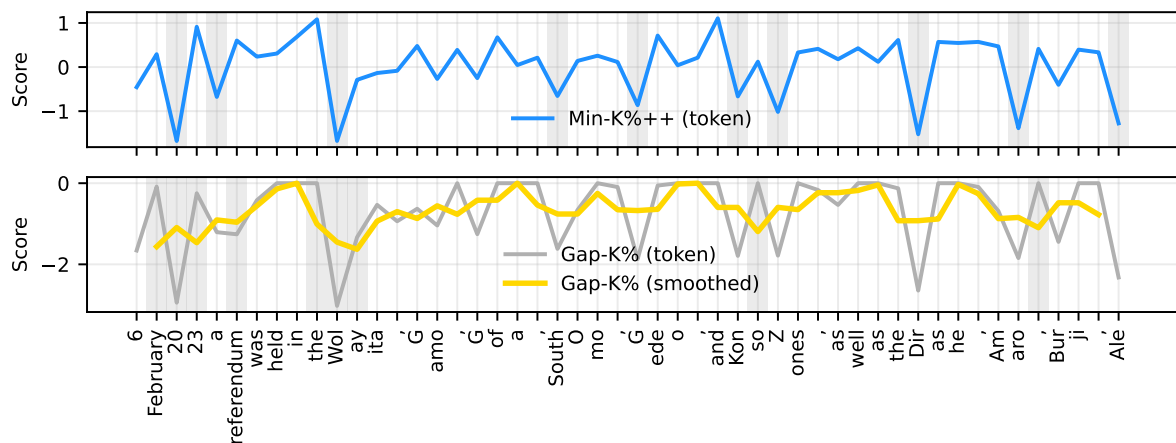
During the preparation of this paper, AI-assisted writing tools were used for editorial purposes,

including improving readability, coherence, and grammatical accuracy. Their use was restricted to language polishing, without generating or altering any technical content. All aspects of the method and experimental outcomes were developed independently by the authors. The application of AI assistance was limited to surface-level revisions and did not affect the originality or scientific substance of the work.

Text: Hurricane Ana was the second tropical cyclone in 2014 to threaten the U.S. state of Hawaii with a direct hit, after Iselle in August. The twenty-first named storm and fifteenth hurricane of



Text: On 6 February 2023 a referendum was held in the Wolayita, Gamo, Gofa, South Omo, Gedeo, and Konso Zones, as well as the Dirashe, Amaro, Burji, Ale, and Basketo special woredas of



Text: A crisis at the National Public Health Laboratory in Khartoum, Sudan, started after it was seized by armed forces during the Sudan conflict in April 2023. The World Health Organization (WHO) said

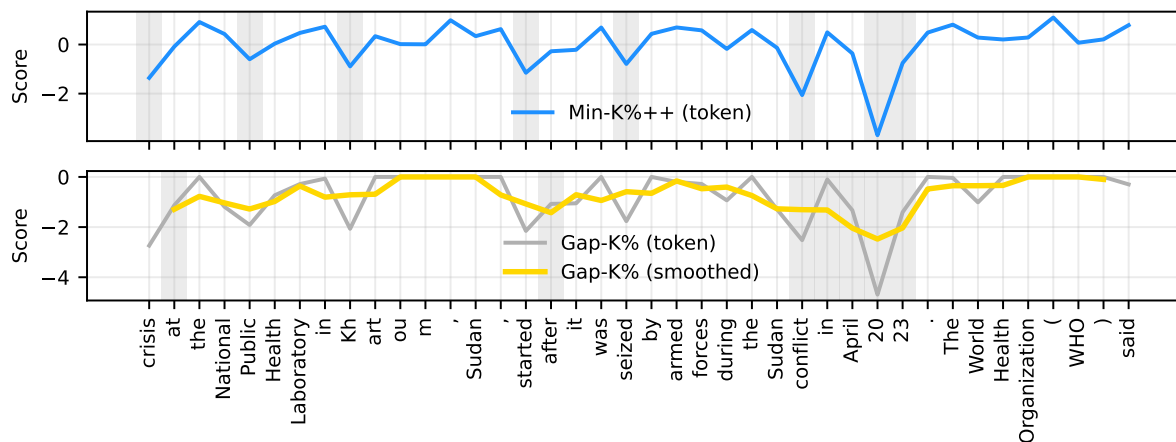


Figure 9: Additional examples of token-level score visualizations for Gap-K% and Min-K%++.